Archives of Biochemistry and Biophysics 702 (2021) 108820

Contents lists available at ScienceDirect

Archives of Biochemistry and Biophysics

journal homepage: www.elsevier.com/locate/yabbi

# Natural diversity of FAD-dependent 4-hydroxybenzoate hydroxylases

Adrie H. Westphal [a], Dirk Tischler [b], Willem J.H. van Berkel [c,*]

[a] Laboratory of Biochemistry, Wageningen University & Research, Wageningen, the Netherlands
[b] Microbial Biotechnology, Faculty of Biology and Biotechnology, Ruhr-Universität Bochum, Germany
[c] Laboratory of Food Chemistry, Wageningen University & Research, Wageningen, the Netherlands

ARTICLE INFO

*Keywords:*
Catabolism
Flavoprotein
4-Hydroxybenzoate
Lignin
Oxygenation
Phylogeny

ABSTRACT

4-Hydroxybenzoate 3-hydroxylase (PHBH) is the most extensively studied group A flavoprotein monooxygenase (FPMO). PHBH is almost exclusively found in prokaryotes, where its induction, usually as a consequence of lignin degradation, results in the regioselective formation of protocatechuate, one of the central intermediates in the global carbon cycle. In this contribution we introduce several less known FAD-dependent 4-hydroxybenzoate hydroxylases. Phylogenetic analysis showed that the enzymes discussed here reside in distinct clades of the group A FPMO family, indicating their separate divergence from a common ancestor. Protein homology modelling revealed that the fungal 4-hydroxybenzoate 3-hydroxylase PhhA is structurally related to phenol hydroxylase (PHHY) and 3-hydroxybenzoate 4-hydroxylase (3HB4H). 4-Hydroxybenzoate 1-hydroxylase (4HB1H) from yeast catalyzes an oxidative decarboxylation reaction and is structurally similar to 3-hydroxybenzoate 6-hydroxylase (3HB6H), salicylate hydroxylase (SALH) and 6-hydroxynicotinate 3-monooxygenase (6HNMO). Genome mining suggests that the 4HB1H activity is widespread in the fungal kingdom and might be responsible for the oxidative decarboxylation of vanillate, an import intermediate in lignin degradation. 4-Hydroxybenzoyl-CoA 1-hydroxylase (PhgA) catalyzes an intramolecular migration reaction (NIH shift) during the three-step conversion of 4-hydroxybenzoate to gentisate in certain *Bacillus* species. PhgA is phylogenetically related to 4-hydroxyphenylacetate 1-hydroxylase (4HPA1H). In summary, this paper shines light on the natural diversity of group A FPMOs that are involved in the aerobic microbial catabolism of 4-hydroxybenzoate.

## 1. Introduction

Lignin is a renewable aromatic plant cell wall polymer, mainly built up from the oxidative coupling of 4-hydroxyphenylpropanoids [1]. Microbial degradation of the heterogeneous lignin macromolecule is initiated by specialized fungi and bacteria, which use extracellular laccases, peroxidases and accessory enzymes to generate a wide range of phenolic breakdown products [2–7]. Subsequent intracellular funneling pathways then converge to a limited number of ring-fission substrates that act as central intermediates in the global carbon cycle [8–10]. Understanding and steering the pathways and enzymes involved in microbial lignin degradation is attractive from a biological, mechanistic and evolutionary point of view, but also relevant for the biobased production of value-added chemicals and the aspiration of a circular economy [2,5,11–13].

4-Hydroxybenzoate (4-HB) is a common intermediate in lignin degradation [6]. It is one of the aromatic acids that arise from the $C_\alpha$-$C_\beta$ cleavage of lignin components [3,14,15]. In aerobic bacteria, 4-HB usually is converted to the ring-fission substrate 3,4-dihydroxybenzoate (protocatechuate, PCA). This reaction, as shown in Fig. 1, is catalyzed by the NAD(P)H-dependent flavoprotein monooxygenase (FPMO) 4-hydroxybenzoate 3-hydroxylase (PHBH; EC 1.14.13.2 [16,17]). The production of PHBH is induced when the microorganism uses 4-HB as carbon source [16].

*Abbreviations:* DTT, dithiothreitol; GA, gentisate (2,5-dihydroxybenzoate); 2-HB, 2-hydroxybenzoate (salicylate); 3-HB, 3-hydroxybenzoate; 4-HB, 4-hydroxybenzoate; HQ, hydroquinone (1,4-dihydroxybenzene); HHQ, hydroxyhydroquinone (1,2,4-trihydroxybenzene); FPMO, flavoprotein monooxygenase; PCA, protocatechuate (3,4-dihydroxybenzoate); PHBH, bacterial 4-hydroxybenzoate 3-hydroxylase; PhhA, fungal 4-hydroxybenzoate 3-hydroxylase; PHHY, phenol hydroxylase from yeast; 3HB4H, 3-hydroxybenzoate 4-hydroxylase; 3HB6H, 3-hydroxybenzoate 6-hydroxylase; 4HB1H, 4-hydroxybenzoate 1-hydroxylase (decarboxylating); HQH, hydroquinone hydroxylase; V1H, vanillate 1-hydroxylase (decarboxylating); SALH, salicylate hydroxylase (decarboxylating); PhgA, 4-hydroxybenzoyl-CoA hydroxylase; 4HPA1H, 4-hydroxyphenylacetate 1-hydroxylase.

* Corresponding author.
*E-mail addresses:* adrie.westphal@wur.nl (A.H. Westphal), dirk.tischler@rub.de (D. Tischler), willem.vanberkel@wur.nl (W.J.H. van Berkel).

https://doi.org/10.1016/j.abb.2021.108820
Received 25 November 2020; Received in revised form 19 February 2021; Accepted 21 February 2021
Available online 5 March 2021

As one of the first flavoenzymes with known crystal structure [18,19], *Pseudomonas* PHBH has developed into a prototype FPMO [20,21]. The catalytic mechanism of PHBH from *Pseudomonas* species has been the subject of extensive research. In the reductive half-reaction, 4-HB and some substrate analogues can act as effectors by stimulating the two-electron reduction of the FAD cofactor by NAD(P)H. In the oxidative half-reaction, the enzyme activates molecular oxygen through formation of a transiently stable flavin C4a-hydroperoxide and subsequently regioselectively incorporates one oxygen atom into the substrate. Based on the structural and kinetic properties of wild-type enzyme and a range of protein variants, the catalytic cycle of PHBH has been proposed to involve flavin movements *in* and *out* of the active site and opening and closure of a substrate transport channel. For details about the different steps of the reaction cycle, we refer to the following review articles [20–23]. Here we focus on the domain structure of PHBH and the binding mode of 4-HB [19].

Fig. 2A shows the 3D-structure of the enzyme-substrate complex of PHBH. Each subunit of the dimeric enzyme contains a split FAD-binding domain (CATH code 3.50.50.60) and a split substrate-binding domain (CATH code 3.30.9.10) [24]. Fig. 2B shows the binding mode of 4-HB. The C3 atom of the aromatic ring of the substrate is in close vicinity of the C4a atom of the isoalloxazine ring of FAD, which occupies the *in* conformation. This active site configuration allows the attack of the flavin C4a-hydroperoxide oxygenation species onto the C3 atom of the substrate. The electrophilic *ortho*-hydroxylation reaction is stimulated by deprotonation of the phenolic moiety of 4-HB, as facilitated by a water involved proton relay network that connects Tyr201 via Tyr385 and His72 with the protein surface [25]. Fig. 2B illustrates that 4-HB is kept in place through a salt-bridge between the carboxylic moiety of the substrate and the guanidinium group of Arg214, and additional H-bond interactions with the hydroxyl moieties of Ser212 and Tyr222 [19]. Fig. 2B also depicts the flavin *out* conformation. This orientation of the isoalloxazine ring is assumed to be needed for flavin reduction [20].

PHBH has been classified as a group A FPMO [26–28]. Group A enzymes are encoded by a single gene, contain a FAD cofactor, and bind the NAD(P)H co-substrate in a groove at the protein surface [29]. Genome mining revealed that PHBHs are mostly present in *Proteobacteria*, while about 10% of these enzymes occur in *Actinobacteria* [29]. It was also established that proteobacterial PHBHs are more specific for NADPH, whereas actinobacterial PHBHs prefer NADH as electron donor [29]. Only few PHBHs were found in the other domains of life, raising the question of how 4-HB is metabolized in *Archaea* and *Eukarya*.

Here we present an overview of the microbial catabolism of 4-HB in aerobic microorganisms. It is shown that 4-HB can be converted to distinct ring-fission substrates through the contribution of different group A FPMOs (Table 1). Phylogenetic analysis revealed that these hydroxylases belong to different clades of the group A FPMO family. For most of these enzymes, the mode of action is poorly understood. Therefore, representatives from three clades were chosen for further investigation. Multiple sequence alignment and protein homology modelling were used to better understand the diversification of these flavoenzymes for their specific function. Next to that, 4HB1H (EC 1.14.13.64) from *Candida parapsilosis* CBS604 was produced as His-tagged protein in *Escherichia coli*, and preliminary characterized.

## 2. Materials and methods

### 2.1. Materials

*Escherichia coli* Top10 strain and pBAD/*Myc*-His vector were obtained from Thermo Fisher Scientific. The gene coding for 4HB1H was purchased from Eurofins Genomics, Germany. 4-Hydroxybenzoate and FAD were purchased from Sigma-Aldrich. All other reagents were of the purest grade commercially available.

### 2.2. Gene cloning and purification of 4HB1H

The codon optimized gene for 4HB1H from *C. parapsilosis* CBS604 (Fig. S1) was cloned into a pBAD/*Myc*-His vector, providing the tail of the gene with a sequence encoding a $His_6$-tag. The obtained plasmid was transformed into *Escherichia coli* Top10 cells. After growing a 3 L culture (6 × 0.5 L LB-medium in 2 L Erlenmeyer flasks with 100 μg/mL ampicillin) of transformed *E. coli* cells at 37 °C in an incubator shaker to an $OD_{600nm}$ of 0.6, protein production was induced by adding arabinose (0.1% final concentration) and incubation continued for another 16 h at 37 °C. After collecting the cells by centrifugation (10.000×*g*, 10 min, 4 °C), the cells were resuspended in 25 mM Tris/Cl buffer, pH 7.8, containing 200 mM NaCl (buffer A), and lysed by sonication using a Q500 sonicator (Qsonica). The obtained extract was cleared by centrifugation (40.000×*g*, 45 min, 4 °C) and loaded on a Ni-NTA metal-affinity column (Cytiva, 2.5 × 10 cm). After washing with buffer A, the protein was eluted with a linear imidazole gradient (0–0.6 M in buffer A, 100 mL) and the active yellow fractions pooled.

After dialysis (10 kDa cut-off membrane; 20 mM Tris/Cl, pH 7.8, containing 10 μM FAD, buffer B), the sample was loaded onto a Source Q ion-exchange column (Cytiva, 2.5 × 10 cm). After washing with buffer B, the protein was eluted with a linear NaCl gradient (0–0.6 M in buffer B, 300 mL) and the active yellow fractions pooled. The sample was concentrated using a spin-filter concentrator (10 kDa cut-off, Millipore) to a volume of 3 mL and loaded on a Superdex-200 (Cytiva) size-exclusion column (2.5 × 100 cm, 20 mM HEPES, 50 mM KCl, pH 7.20, containing 10 μM FAD). Fractions containing the main yellow peak were concentrated again using a spin-filter concentrator (10 kDa cut-off) to a volume of 3 mL. The sample was aliquoted (0.5 mL), flash frozen with liquid $N_2$ and stored at −80 °C. Lipid content determination was performed as described in Ref. [30]. 3-Hydroxybenzoate 6-hydroxylase (3HB6H; EC 1.14.13.24) from *Rhodococcus jostii* RHA1 was used as a lipid-containing reference protein, which was prepared as described previously [31].

### 2.3. Activity measurements of 4HB1H

4HB1H activity was measured by following the decrease of absorbance due to enzymatic oxidation of NADH at 340 nm and 25 °C. The assay mixture contained 0.1 mM 4-HB, 0.2 mM NADH, and 10 μM FAD in air-saturated 50 mM potassium phosphate (pH 7.6). The addition of FAD was essential to achieve optimal turnover. One unit of enzyme is defined as the amount that catalyzes the oxidation of 1 μmole of NADH per min under the assay conditions. The used molar absorption coefficient for NADH at 340 nm was 6.22 $mM^{-1}$ $cm^{-1}$ 4HB1H-catalyzed formation of 1,4-dihydroxybenzene (hydroquinone; HQ) was checked by following the disappearance in absorption of 4-HB at 250 nm [32].

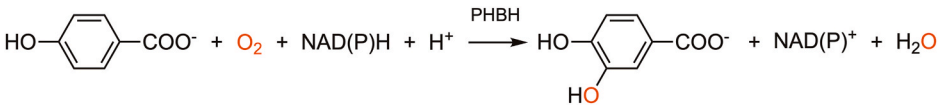


**Fig. 1.** PHBH-mediated hydroxylation of 4-HB to ring-fission substrate PCA.

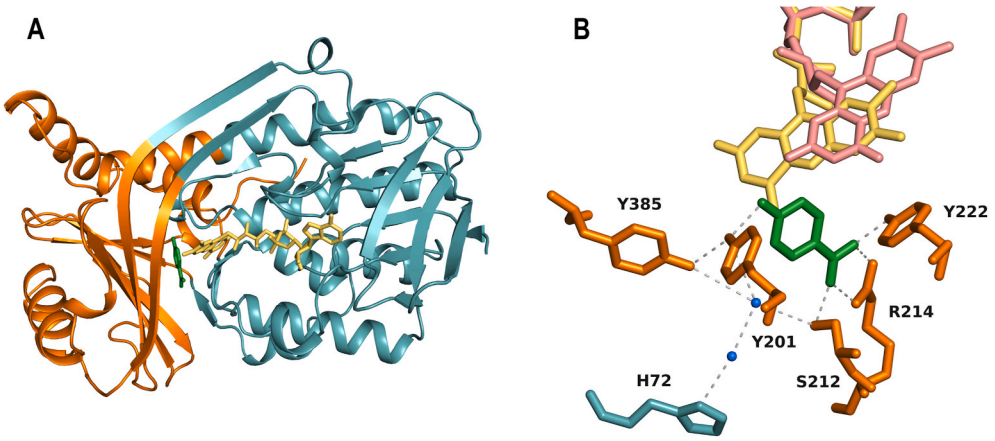


**Fig. 2.** Crystal structure of PHBH from *Pseudomonas fluorescens*. A) Overall protein fold of the PHBH subunit (pdb:1pbe). The FAD-binding domain is indicated in blue, the FAD cofactor in yellow, the substrate-binding domain in orange, and 4-HB in green. B) Binding-mode of 4-HB. The isoalloxazine ring of the flavin is indicated in yellow (*in* conformation) and pink (*out* conformation), the substrate in green, and the amino acid residues in corresponding domain color. Two water molecules are indicated by blue spheres. (For interpretation of the references to color in this figure legend, the reader is referred to the Web version of this article.)

**Table 1**
Group A FPMOs involved in the microbial catabolism of 4-hydroxybenzoate.

| Gene | Source | Enzyme | Substrate | Product |
|---|---|---|---|---|
| *pob*A | bacterium | PHBH | 4-hydroxybenzoate | 3,4-dihydroxybenzoate (protocatechuate) |
| *phh*A | fungus | PhhA | 4-hydroxybenzoate | 3,4-dihydroxybenzoate (protocatechuate) |
| *mnx*1 | yeast | 4HB1H | 4-hydroxybenzoate | 1,4-dihydroxybenzene (hydroquinone) |
| *mnx*3 | yeast | HQH | 1,4-dihydroxybenzene (hydroquinone) | 1,2,4-trihydroxybenzene (hydroxyhydroquinone) |
| *v1h* | fungus | V1H | 4-hydroxy-3-methoxybenzoate | methoxyhydroquinone |
| *phg*A | bacterium | PhgA | 4-hydroxybenzoyl-CoA | 2,5-dihydroxybenzoyl-CoA (gentisyl-CoA) |

[1]Abbreviations: PHBH, bacterial 4-hydroxybenzoate 3-hydroxylase; PhhA, fungal 4-hydroxybenzoate 3-hydroxylase; 4HB1H, 4-hydroxybenzoate 1-hydroxylase (decarboxylating) from yeast; HQH, hydroquinone hydroxylase; V1H, putative vanillate 1-hydroxylase (decarboxylating); PhgA, 4-hydroxybenzoyl-CoA hydroxylase.

### 2.4. SDS-PAGE and protein determination

Sodium dodecyl sulfate-polyacrylamide gel electrophoresis (SDS-PAGE) was used for protein visualization. Samples were mixed with 4x Bolt LDS sample buffer (Thermo Fisher Scientific) and loaded on a 15-wells Bolt gradient Bis-Tris Mini Protein Gel (Thermo Fisher Scientific). Samples were incubated at 80 °C in the presence or absence of 10 mM dithiothreitol (DTT) before loading. Precision Plus Protein Dual Color Standards (Bio-Rad) was used as marker and gels were stained for 2 h in a 30% ethanol solution, containing 8% acetic acid and 0.05% (w/v) Coomassie brilliant blue. Destaining was performed in demineralized water overnight.

Protein concentration was determined using a Pierce BCA Protein Assay Kit (Thermo Fisher Scientific) according to suppliers' instructions.

### 2.5. Phylogenetic analysis of group A enzymes

88 amino acid sequences of distinct group A FPMOs were taken from UniProt or NCBI. These were aligned by means of ClustalW in MEGA 7 and MEGA 10 [33] using the standard setup. The alignment was subjected to a phylogenetic analysis prior generating the phylogenetic distance tree. Therefore, the Neighbor-Joining method was employed [34], while the evolutionary distances were computed using the JTT matrix-based method [34,35]. For statistical reasons we employed the Bootstrap method with 1000 replicates [36]. The same result was used to show a radial tree pointing out the evolutionary history. For presentation reasons the Bootstrap values were eliminated in this case and some branches were collapsed to form bigger clades while a representative enzyme designation is given.

### 2.6. Protein homology modelling

An alignment of the amino acid sequences of An_PhhA and Tc_PHHY was made using the program Promals3D [37]. This alignment, together with the structure file of Tc_PHHY (PDB: 1pn0) as template, were provided as input for constructing models using the program Modeller version 9.25 [38]. For each modelling run, four hundred comparative models were generated, after which the model with lowest corresponding DOPE score [39] was selected for images generation using Pymol [40]. Using the same procedure, Tc_PHHY (pdb: 1pn0) was also used as template structure for the generation of a model of Cp_HQH. Models for Cp_4HB1H, Fo_4HB1H-like, and VibMO1 were generated using Rj_3HB6H (pdb: 4bk1) and Pp_SALH (pbd: 5evy) as template structures. The FAD cofactor was included in all modelling runs. Substrates present in the template structures were manually replaced with the structures of the actual substrates, resulting in models containing the FAD and aromatic substrate molecules. Because of the presence of multiple charged and flexible side chains in the active sites of the generated models, and the inherent inaccuracy of their exact conformations and charge status, docking of aromatic substrates into the models was not performed.

## 3. Results

### 3.1. Phylogenetic analysis of group A FPMOs

To get insight into the evolutionary relationship between the NAD(P)H-dependent FAD-containing 4-hydroxybenzoate hydroxylases described in the current study, we performed a phylogenetic analysis of group A FPMOs that have been (partially) characterized. In total, 88 different enzymes with a distinct physiological function were taken into consideration, excluding the modular MICAL proteins (EC 1.14.13.225), which modulate cell shape and motility in eukaryotes [41]. In addition, we used 5 sequences of FPMOs from group E and F as an outgroup to make the analysis more robust, as was done previously for group A FPMOs with known structure [24]. A bootstrap consensus tree with enzyme names, UniProt numbers and PDB identification codes is presented in Fig. S2.

From the condensed consensus tree depicted in Fig. 3, it can be seen that the bacterial PHBHs cluster in a separate clade (indicated in orange), and that they are distantly related to the fungal 4-hydroxybenzoate 3-hydroxylase PhhA (blue clade). The latter enzyme clusters together with several *ortho*-hydroxylases, including phenol hydroxylase (PHHY; EC 1.14.13.7) from *Trichosporon cutaneum*, hydroquinone hydroxylase (HQH) from *C. parapsilosis* and 3-hydroxybenzoate 4-

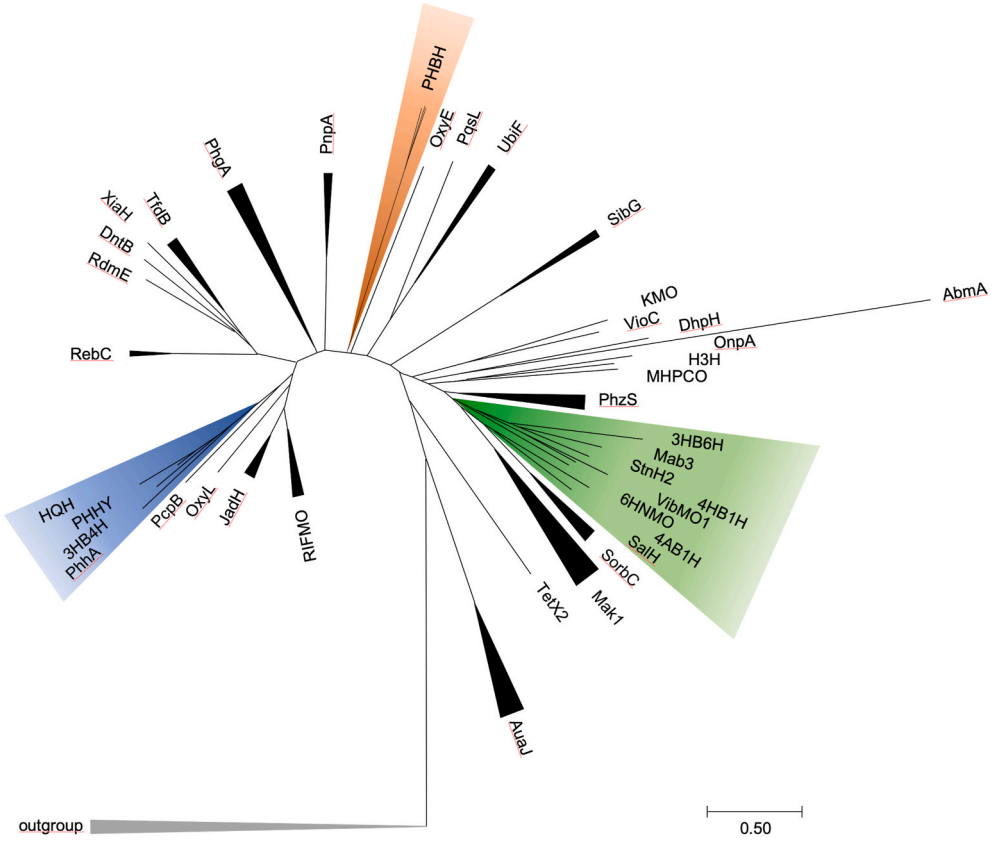


**Fig. 3.** Condensed bootstrap consensus tree of group A FPMOs.

hydroxylase (3HB4H; EC 1.14.13.23) from *Comamonas testosteroni*. 4HB1H on the other hand, is found in another part of the tree (green clade) and clusters together with several decarboxylating hydroxylases, including fungal 4-aminobenzoate 1-hydroxylase (4AB1H; EC 1.14.13.27) and the bacterial enzymes SALH, VibMO1 and 6-hydroxynicotinate 3-monooxygenase (6HNMO; EC 1.14.13.114). This cluster also houses several bacterial *para*-hydroxylases, including 3-aminobenzoate 6-hydroxylase (Mab3), 3-hydroxy-2-aminobenzoate 6-hydroxylase (StnH2) and 3HB6H.

### 3.2. Conversion of 4-hydroxybenzoate (4-HB) to protocatechuate (PCA)

As mentioned in the Introduction, PHBH is almost exclusively found in bacterial phyla [29]. Certain ascomycetous fungi also convert 4-HB to PCA, but the responsible enzyme, referred to as PhhA, was reported to have 'nebulous' sequence homology with PHBH [10,42]. Expression of PhhA from *Aspergillus niger* N402 in *E. coli* was unsuccessful, but the enzyme could be produced in *A. niger* N593 [43]. Although the enzyme activity was lost upon purification, it was confirmed that the recombinant PhhA converted 4-HB into PCA. It was also reported that the *phhA* gene is conserved in ascomycete genomes and that PhhA has significant amino acid sequence similarity with 3HB4H from *C. testosteroni*, but is not active with 3-hydroxybenzoate (3-HB) [43]. These findings prompted us to generate a protein homology model of PhhA and take a closer look at its active site.

A structure-based multiple sequence alignment confirmed that PhhA is structurally related to PHHY from *T. cutaneum* (pdb: 1pn0 [44,45]) and to 3HB4H from *C. testosteroni* (pdb: 2dkh [46]) (Fig. 4). Both these homodimers contain, in addition to the split FAD- and substrate-binding domains, a C-terminal thioredoxin-like domain (CATH code 3.40.30.20) that forms part of the dimer interface. From the sequence alignment in Fig. 4, it is evident that PhhA with 622 amino acid residues also contains this extra domain. Furthermore, PhhA and 3HB4H are missing a flexible loop, which is, in PHHY (residues 170–206), involved in flavin movement and closing-off the active site.

PHBH, PHHY and 3HB4H all catalyze *ortho*-hydroxylation reactions. However, the orientation of the phenolic substrates in PHHY and 3HB4H is different from the orientation of 4-HB in PHBH. Tyr222 interacts in PHBH with the carboxy moiety of 4HB (Fig. 2B), while in PHHY and 3HB4H, this conserved tyrosine makes a hydrogen bond with the hydroxyl group of the phenolic substrates [44,46]. To better understand the reactivity of PhhA with 4HB, we constructed a homology model of its three-dimensional structure (Fig. 5) and analysed the possible mode of substrate binding.

The substrate binding pockets of PhhA, PHHY and 3HB4H are shown in Fig. 6. Besides from the conserved tyrosine, there is a conserved aspartate that interacts with the hydroxyl group of the substrate. For PHHY (Fig. 6B), it was shown that replacement of Asp54 with Asn results in inefficient substrate hydroxylation and that Tyr289 is critical for rapid flavin reduction by NADPH, presumably through facilitating the flavin *out* conformation [47]. For 3HB4H, no mutations of Asp75 and Tyr271 were made, but based on their positions in the enzyme-substrate complex (Fig. 6C), it was argued that Asp75 and Tyr271 might enhance the electron donating capacity of the hydroxyl group of 3-HB [46].

In 3HB4H, the carboxyl group of 3-HB preferentially interacts with the side chains of His135 and Lys247 (Fig. 6C). This ionic interaction was proposed to determine the orientation of bound substrate [46]. Interestingly, a directed evolution study revealed that 3HB4H from *C. testosteroni* GZ39 is considerably active with 4-HB and that this activity increases in the V257A variant [48]. The same variant slowly converted phenol to catechol, an activity not observed with the wild-type enzyme.

In PHHY (Fig. 6B), the side chain of Gln112 is very close to the C4-atom of phenol, which might explain why 4-HB is not accepted as substrate [49]. The active site model of PhhA (Fig. 6A) suggests that Thr111 and Lys219 are key to the proper orientation of the aromatic ring of

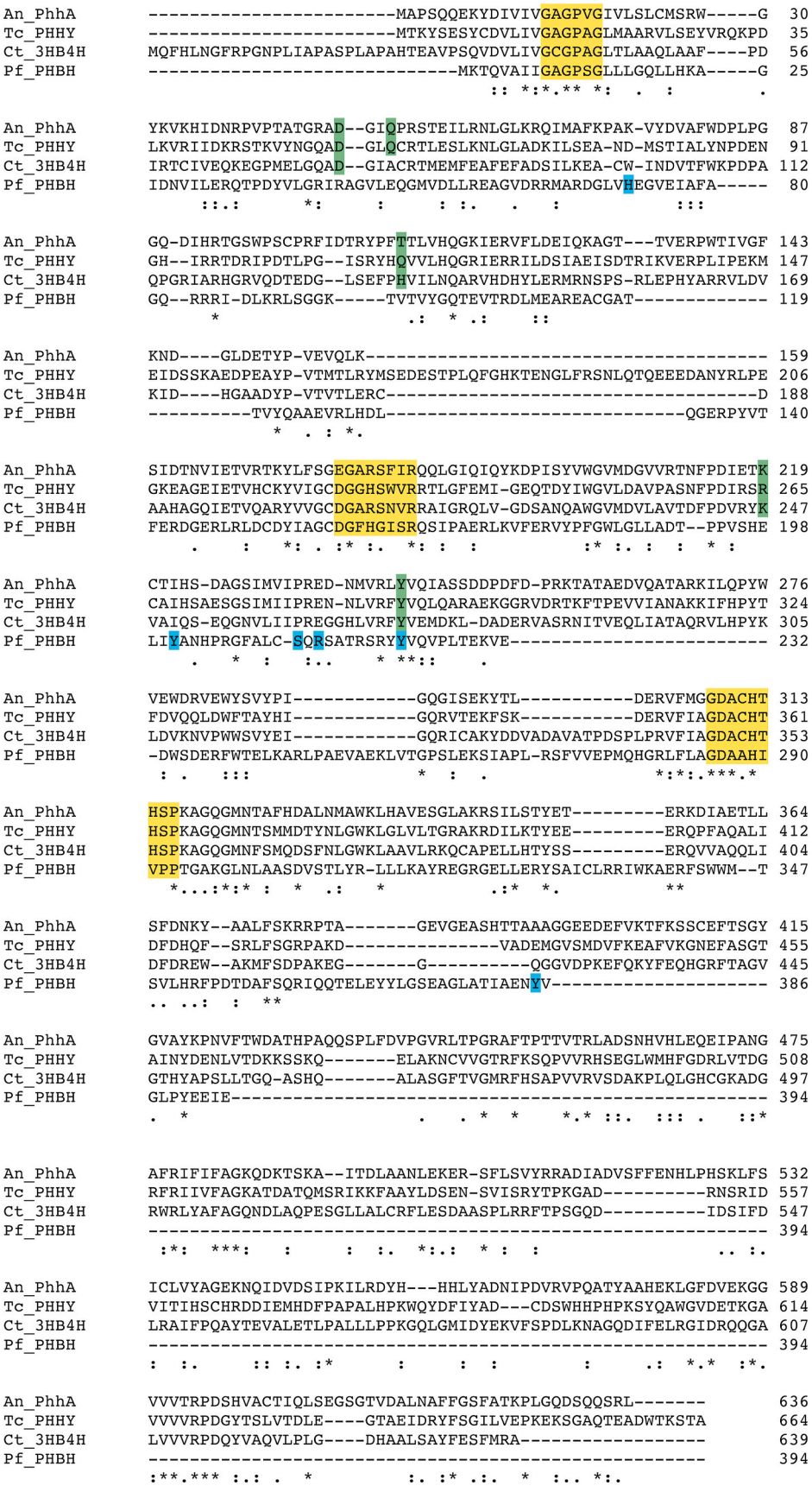


**Fig. 4.** Stucture-based multiple sequence alignment of PhhA from *A. niger* N402 with PHHY from *Trichosporon cutaneum* (UniProt sequence P15245 corrected according to Refs. [44,45], 3HB4H from *C. testosteroni,* and PHBH from *P. fluorescens* (sequence identities respectively 35.2, 32.7 and 21.0%). FAD fingerprints are marked in yellow, active site residues of PhhA, PHHY and 3HB4H in green, and active site residues of PHBH in blue. Numbering of PhhA is corresponding to PHHY in its structure file pdb:1pn0. (For interpretation of the references to color in this figure legend, the reader is referred to the Web version of this article.)

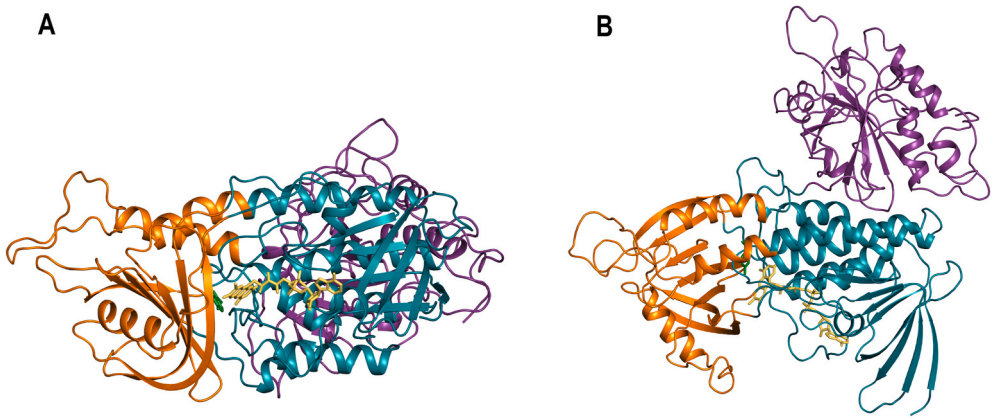


**Fig. 5.** Protein homology model of PhhA from *A. niger* N402. A) Overall protein fold of the modelled PhhA subunit. The FAD-binding domain is indicated in teal, the FAD cofactor in yellow, the substrate-binding domain in orange, the thioredoxin domain in purple and 4-HB in green. B) Rotated view of the modelled PhhA, clearly showing the thioredoxin domain. (For interpretation of the references to color in this figure legend, the reader is referred to the Web version of this article.)

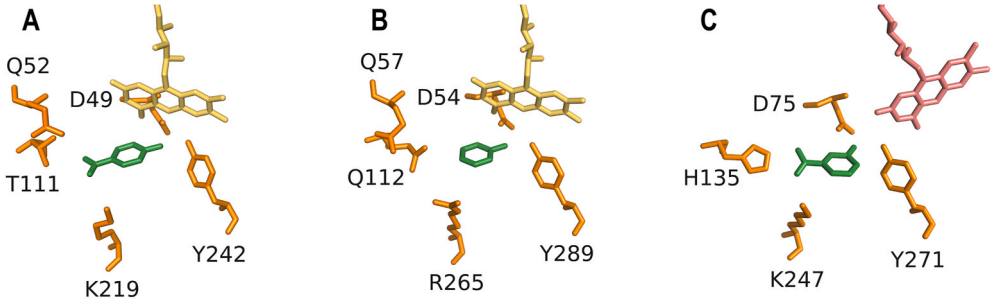


**Fig. 6.** Substrate binding pockets of PhhA (left, A), PHHY (middle, B) and 3HB4H (right, C). The *in* conformation of the flavin cofactor is indicated in yellow and the *out* conformation in pink. 4-HB was positioned in the PhhA structural model in a similar orientation as the phenolic substrates in PHHY (pdb: 1pn0) and 3HB4H (pdb: 2dkh). (For interpretation of the references to color in this figure legend, the reader is referred to the Web version of this article.)

4-HB, which would explain why PhhA is not active with 3-HB. Because functional predictions based on homology are challenging, it is evident that additional experimental work is required to better understand the substrate specificity of this novel fungal group A FPMO.

### 3.3. Conversion of 4-hydroxybenzoate (4-HB) to hydroquinone (HQ)

In 1994, we reported that the ascomycetous yeast *Candida parapsilosis* CBS604 converts 4-HB to HQ and that in the subsequent step, HQ is converted to the ring-fission substrate 1,2,4-trihydroxybenzene (hydroxyhydroquinone; HHQ) (Fig. 7A [32]).

Enzyme purification revealed that both steps are catalyzed by FAD-dependent monooxygenases [50,51]. The monomeric 4HB1H, responsible for the first step, was shown to catalyze the oxidative decarboxylation of a wide range of 4-HB derivatives. Based on this and molecular orbital calculations it was proposed that the conversion of 4-HB involves an *ipso*-attack of the electrophilic flavin C4a-hydroperoxide at the C1-atom of the activated substrate, resulting in a tetrahedral

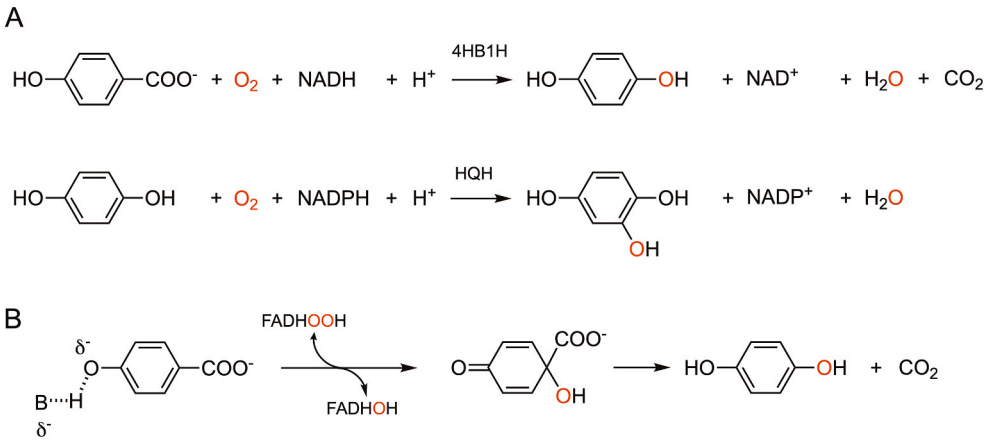


**Fig. 7.** Initial steps of the catabolism of 4-HB in *C. parapsilosis* CBS604. A) The conversion of 4-HB to HQ is catalyzed by the NADH-preferring 4HB1H, whereas the conversion of HQ to HHQ is catalyzed by the NADPH-preferring HQH. B) Proposed reaction scheme for the flavin-hydroperoxide stimulated hydroxylation of 4-HB to HQ by 4HB1H [50].

benzoquinone species and subsequent release of the carboxyl side chain (Fig. 7B) [50]. The second step of the catabolism of 4-HB in *C. parapsilosis* CBS604 (Fig. 7A) was shown to be catalyzed by the homodimeric HQH that has catalytic and structural properties in common with PHHY from *T. cutaneum* [51].

The genome of *C. parapsilosis* CBS604 was sequenced in 2009 [52]. This allowed the search for candidate genes involved in the degradation of 4-HB. It was found that the *mnx1* and *mnx3* genes code for 4HB1H and HQH, respectively, and that only a limited amount of *Candida* species and related saccharomycetes contain these genes [53,54].

Sequence alignment confirmed that HQH from *C. parapsilosis* CBS604 is closely related to PHHY from *T. cutaneum* (Fig. S3; 43.4% sequence identity). Most residues involved in substrate binding are strictly conserved, and HQH also contains the flexible loop that in PHHY closes off the active site [44]. A model of the substrate binding site of HQH is presented in the supplementary information (Fig. S4).

A structure-based multiple sequence alignment (Fig. 8) suggested that 4HB1H from *C. parapsilosis* CBS604 is structurally related to 3HB6H from *R. jostii* RHA1 (pdb: 4bk1) [30] and SALH (EC 1.14.13.1) from *Pseudomonas putida* G7 (pdb: 5evy) [55,56]. However, 4HB1H is unique among these proteins in having a much longer C-terminal tail.

4HB1H was produced as C-terminally His-tagged protein in *E. coli* Top10 cells (see Materials & Methods). About 10 mg 4HB1H per litre of culture could be purified using Ni-NTA metal affinity chromatograph followed by ion-exchange and size-exclusion chromatography. According to SDS-PAGE, the purification resulted in a protein with an apparent molecular mass of 55 kDa (Fig. S5).

Size-exclusion chromatography confirmed the earlier finding [50] that in solution, the enzyme is a monomer. The UV–Vis absorption spectrum of 4HB1H revealed typical flavoprotein features, with absorption maxima at 375 nm and 450 nm. Activity measurements with 4-HB as substrate and NADH as co-substrate showed an almost complete disappearance of the absorption at 250 nm, consistent with the formation of HQ [32]. The specific activity of 14 ± 1 U/mg, as determined by the decrease in absorption at 340 nm, was in good agreement with the specific activity of 12 ± 1 U/mg reported for the enzyme isolated from *C. parapsilosis* [50]. Kinetic studies with the *C. parapsilosis* enzyme have established that 4HB1H is active with a wide range of 4-HB derivatives with $k_{cat}$ and $K_M$ values similar to that found for 4-HB ($k_{cat}$ = 10 $s^{-1}$; $K_M$ = 10 μM) [50].

```
Cp_4HB1H      MAVQAPSKTYGFQKAPIQLTFVVVGAGLGGVAASICLRLAGH-RVILLEAATEL--GEVG 57
Pp_SALH       -------------MSKSPLRVAVIGGGIAGTALALGLSKSSHVNVKLFETAPAF--GEIG 45
Rj_3HB6H      ------------MSNLQDARIIIAGGGIGGAANALALAQKGA-NVTLFERASEF--GEVG 45
Pf_PHBH       ----------------MKTQVAIIGAGPSGLLLGQLLHKAGIDNVILERQTPDYVLGRIR 44
                             . : *.* .*   .  *   .  .* * . :     *.:

Cp_4HB1H      AGIQIPPPSTKILKAIGVLDAVDKVSIHPHD----ILV--K--KYKGELLSTQNLVPYVS 109
Pp_SALH       AGVSFGVNAVEAIQRLGIGELYKSVADSTPAPWQDIWFEWR-HAHDASLVGA-------T 97
Rj_3HB6H      AGLQVGPHGARILDSWGVLDDVLSRAFLPKN----IVF--R-DAITAEVLTKIDLGSEFR 98
Pf_PHBH       AGVLEQ-GMVDLLREAGVDRRMARDGLV-HE-GVEIAFAGQRRRIDLKRLSGGKTV---- 97
              **:      .  :   *:       .         * .  :      . :

Cp_4HB1H      EKYDGMYLHIHRADYHKVLVDRAEELGVE-IHTNSRVVDIDF--EKATVTTATG---KQY 163
Pp_SALH       VAPGIGQSSIHRADFIDMLEKRLPAGIA---SLGKHVVDYTENAEGVTLNFADG---STY 151
Rj_3HB6H      GRYGGPYFVTHRSDLHATLVDAARAAGAE-LHTGVTVTDVITEGDKAIVSTDDG---RTH 154
Pf_PHBH       -------TVYGQTEVTRDLMEAREACGATTVYQAAEVRLHDLQGERPYVTFERDGERLRL 150
                         :::    * .      .        *       :   :.   .

Cp_4HB1H      SGDVIVGYDGVRSQTRALLTGD----SSGAYDTGDLAYRALIKVEDMKKVPGLE---KFY 216
Pp_SALH       TADVAIAADGIKSSMRNTLLRAAGHDAVHPQFTGTSAYRGLVETSALREAYQAASLDEHL 211
Rj_3HB6H      EADIALGMDGLKSRLREKISGD------EPVSSGYAAYRGTTPYRDVELDEDIE------ 202
Pf_PHBH       DCDYIAGCDGFHGISRQSIPAE---------------------------------RLKVF 177
                *   . **.:.  *  :

Cp_4HB1H      ANPNINFWWG------PTMHIVMYFLHEGEICNVVALCPDTLPKG--------------- 255
Pp_SALH       -LNVPQMYLI------EDGHVLTFPVKKGKLIIIVAFVSDRSVAKP-------------Q 251
Rj_3HB6H      ---DVVGYIG------PRCHFIQYPLRGGEMLNQVAVFESPGFKN--------------- 238
Pf_PHBH       ERVYPFGWLGLLADTPPVSHELIYANHPR----GFALCSQRSATRSRYYVQVPLTEKVED 233
                     :           * : :  :       .*.  .

Cp_4HB1H      -----VLKQDASQEELLDLVKGWDQDLTTVFKLITSVSKWRLQDSRELKTWVN--SKTGN 308
Pp_SALH       WPSDQPWVRPATTDEMLHRFAGAGEAVKTLLTSIKSPTLWALHDFDPLPTYVH-----GR 306
Rj_3HB6H      -----GIENWGGPEELEQAYAHCHENVRRGIDYLWKDRWWPMYDREPIENWVD-----GR 288
Pf_PHBH       WSDERFWTELKA-----RLPAEVAEKLVTGPSLEKS--------IAPLRSFVVEPMQHGR 280
                       .               : :       .          : .:*      *.

Cp_4HB1H      FIILGDASHSTLPYLASGASQAVEDGAVLAGLFSKIES---RDQIPQLLQMTEN---LRK 362
Pp_SALH       VALIGDAAHAMLPHQGAGAGQGLEDAYFMAELLGNPLH--EASDIPALLEVYDD---VRR 361
Rj_3HB6H      MILLGDAAHPPLQYLASGAVMAIEDAKCLADYAAEDFSTGGNSAWPQILKEVNT---ERA 345
Pf_PHBH       LFLAGDAAHIVPPTGAKGLNLAASDVSTLYRLLLKAYREGRG----ELLERYSAICLRRI 336
              . : ***:*      . *   . .*   :     :            :*:  .     *

Cp_4HB1H      WRSSQVVRGSHQCQDIYHLPDGELQEIRDSYLYDKQPELGCPNRFADPVFQDFLWGYNAF 422
Pp_SALH       GRASKVQLTSREAGELYEYRTPGVERDT------------AKLKALLESRMNWIWNYDLG 409
Rj_3HB6H      PRCNRILTTGRMWGELWHLDGTARI---------ARNELFRTRDTSSYKYTDWLWGYSSD 396
Pf_PHBH       WKAERFSW--WMTSVLHRFPDTDAF---------------------SQRIQQTELEYYLG 373
               :..:.         : .                                :    *

Cp_4HB1H      DEVERAWKEFKAGGNPTYTYPNLYKPKSSGEKDVSGGGAAATLAAGNTPAAPLSASG    479
Pp_SALH       AEARLAVKPALA-------------------------------------------    421
Rj_3HB6H      RAS----------------------------------------------------    399
Pf_PHBH       SEAGLATIAENYVGLPYEEIE----------------------------------    394
```

**Fig. 8.** Structure-based multiple sequence alignment of 4HB1H from *C. parapsilosis* CBS604 (UniProt: G8B709) with SALH from *P. putida* G7, 3HB6H from *R. jostii* RHA1 and PHBH from *P. fluorescens* (sequence identities respectively 25.8, 30.5 and 23.2%). FAD fingerprints are marked in yellow, active site residues of 4HB1H, SALH and 3HB6H in green, and active site residues of PHBH in blue. (For interpretation of the references to color in this figure legend, the reader is referred to the Web version of this article.)

Samples of the purified recombinant 4HB1H showed two closely spaced bands on SDS-PAGE (Fig. S5). However, pre-incubation of the protein with DTT before SDS-PAGE resulted in a single band on SDS-PAGE, indicating the presence of (an) oxidized cysteine(s), affecting electrophoretic behaviour (Fig. S5). Attempts to crystallize the enzyme thus far failed. We therefore constructed a homology model of its three-dimensional structure and compared the possible mode of substrate binding with those of SALH and 3HB6H (Fig. 9).

Mass spectrometry analysis revealed that 4HB1H does not contain a lipid cofactor as observed for 3HB6H [31]. This phospholipid has been proposed to be important for orienting the 3-HB substrate of 3HB6H for regioselective hydroxylation at C6 [30]. The absence of a corresponding lipid and the fact that both 4HB1H and SALH catalyze an oxidative decarboxylation reaction might suggest that the mode of binding of 4-HB in 4HB1H resembles that of 2-HB in SALH. Based on this assumption we positioned 4-HB in the structural model of 4HB1H in a similar orientation as the 2-HB substrate in SALH (Fig. 8). Tyr379 and Tyr94 can make in this orientation a hydrogen bond to the hydroxyl group of 4-HB, thereby possibly stimulating substrate activation.

For SalH, it was disputed if Ser49 [55] or His224 [56] functions as active site base, whereas for 3HB6H it was established that His213 serves this role [57,58] (Fig. 8). Without structural and/or mutagenesis data, it cannot be excluded that His230 activates 4-HB in 4HB1H for *ipso*-attack by the flavin C4a-hydroperoxide. Furthermore, it can also not be ruled out that the substrate of 4HB1H binds in a flipped orientation with the 4-hydroxyl moiety pointing towards the side chains of Tyr116 and His118. Based on results from site-directed mutagenesis, such a mode of binding was recently proposed for the related 6-hydroxynicotinate 3-monooxygenase from *Bordetella bronchiseptica* RB50 (6HNMO; EC 1.14.13.114) [59]. Strikingly, previous docking of 6-hydroxynicotinate into the structure of 6HNMO from *P. putida* KT2440 (pdb: 5eow) led to the conclusion that His211 (equivalent to His230 in 4HB1H) might serve as the general base catalyst [60], underlining the complexity of predicting correctly the mode of substrate binding in group A FPMOs on the basis of closest structural homologs.

4HB1H efficiently converts vanillate (4-hydroxy-3-methoxybenzoate) to methoxy-hydroquinone [50]. Early studies on lignin biodegradation suggested that the vanillate 1-hydroxylase (V1H) activity is widely distributed in brown-rot and white-rot basidiomycetes [61–63] and that the involved NAD(P)H-dependent flavoenzyme is also active with 4-HB [64]. However, the gene coding for V1H has never been assigned. This is fairly surprising since vanillate is, next to 4-HB, one of the most cited monoaromatic compounds in lignin biodegradation studies [6].

As mentioned above, 4HB1H is only present in a small group of saccharomycetes. However, we noticed that a wide range of FAD-binding proteins from pezizomycetes and agaricomycetes with unknown function have significant sequence identity (up to 39.5%) with 4HB1H, raising the possibility that they are responsible for the V1H and 4HB1H activities in these strains. These 4HB1H-like proteins (for instance UniProt F9F4T0 from *Fusarium oxysporum* and UniProt K5W700_from *Phanerochaete carnosa* HHB10118) are a bit shorter in sequence than 4HB1H and their active site residues are quite comparable to those of 4HB1H and 3HB6H (Fig. S6). For comparison, Fig. S7 shows an active site model of the 4HB1H-like protein from *F. oxysporum*, in which we positioned 4-HB in a similar orientation as 3-HB in 3HB6H.

Worth mentioning here is that the FAD-dependent monooxgenase VibMO1 converts 3-prenyl-4-hydroxybenzoate into prenylhydroquinone. VibMO1 has been proposed to be involved in the biosynthesis of vibralactones and other meroterpenoids in the basidiomycete *Boreostereum vibrans* [65]. Bv_VibMO1 (Uniprot: A0A167KUL3) shows 44.7% sequence identity with Cp_4HB1H and most residues involved in substrate binding in 4HB1H are conserved in the Bv_VibMO1 sequence (Fig. S8). Furthermore, Bv_VibMO1 is active with 4-HB [65].

In conclusion, more knowledge about the structure-function relationship of decarboxylating 4-hydroxybenzoate hydroxylases is highly desirable. This is underscored by the fact that related group A FPMOs are crucially involved in the biosynthesis of coenzyme Q and plant prenyl (hydro)quinone derivatives [65], and in the detoxification of halogenated 4-hydroxybenzoates in marine organisms [66].

### 3.4. Conversion of 4-hydroxybenzoate (4-HB) to gentisate (GA)

Besides the *ortho*- and *para*-hydroxylation reactions described above,

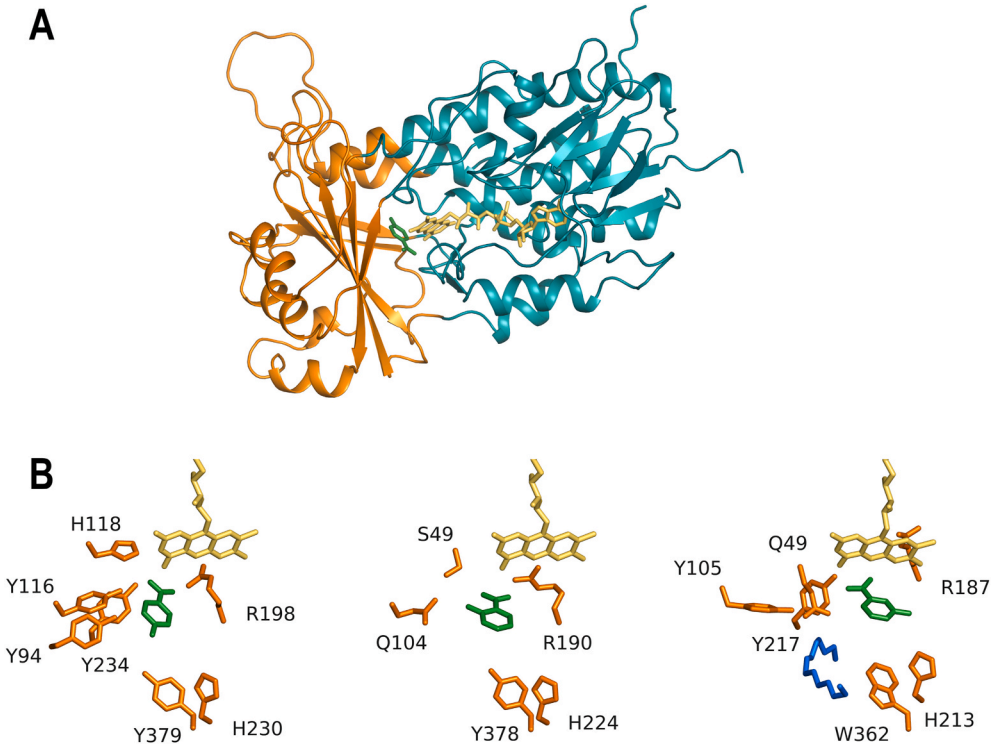


**Fig. 9.** Protein homology model of 4HB1H from *C. parapsilosis* CBS604. A) Overall protein fold of the modelled 4HB1H. The FAD-binding domain is indicated in teal, the FAD cofactor in yellow, the substrate-binding domain in orange and 4-HB in green. B) Comparison of the substrate binding pockets of 4HB1H (left), SALH (middle) and 3HB6H (right). The *in* conformation of the flavin cofactors are indicated in yellow and the substrates in green. 4-HB is positioned in the 4HB1H structural model in a similar orientation as the 2-HB substrate in SALH (pdb: 5evy). Part of the lipid, protruding into the active site pocket of 3HB6H (pdb:4bk1), is colored blue. (For interpretation of the references to color in this figure legend, the reader is referred to the Web version of this article.)

4-HB can also be hydroxylated through a NIH-shift mechanism. This reaction, first discovered in *Brevibacillus laterosporus* PHB-7a [67] involves introduction of a hydroxyl group at the *para* position of 4-HB and subsequent intramolecular migration of the carboxyl group (1,2-shift), yielding 2,5-dihydroxybenzoate (gentisate, GA). Based on studies with the haloarchaeal *Haloarcula* sp. strain D1, it was postulated that the migration reaction requires the intermediate formation of a CoA thioester [68]. Only recently, the molecular basis for this mechanism was laid by Zhou and coworkers [69]. From performing bioinformatics, transcriptomics, molecular cloning and stable isotopic experiments they were able to demonstrate that the *phg*ABC genes of the 4-HB utilizing *B. laterosporus* PHB-7a encode a 4-hydroxybenzoyl-CoA ligase (PhgC), a 4-hydroxybenzoyl-CoA 1-hydroxylase (PhgA), and a gentisyl-CoA thioesterase (PhgB) for the three-step conversion of 4-HB to GA, as shown in Fig. 10.

PhgA, responsible for the *para*-hydroxylation of 4-hydroxybenzoyl-CoA and the 1,2-shift of the acyl-CoA moiety (Fig. 10B), was found to be a group A FPMO having less than 30% sequence identity with other group members. PhgA is phylogenetically closely related with 4-hydroxyphenylacetate 1-hydroxylase (4HPA1H; EC 1.14.13.18) (Fig. S1). Interestingly, 4HPA1H also catalyzes a 1,2-shift migration reaction, thereby producing 2,5-dihydroxyphenylacetate (homogentisate) [70]. PhgA has certain structural features in common with rifampicin monooxygenase (RIFMO; EC 1.14.13.211; pdb: 5kow) but lacks the C-terminal thioredoxin-like domain (Fig. S9). The active site of RIFMO has a large groove, capable of binding the bulky rifampicin substrate [71,72]. Such an open active site might also be needed for binding 4-hydroxybenzoyl-CoA and would explain why PhgA does not accept 4-HB as substrate [69].

Genome analysis revealed that the *phg*A gene cluster is only present in a selected group of *Bacillus* species that do not contain *pob*A genes [69]. Because 4-hydroxybenzoyl-CoA is a common intermediate in anaerobic aromatic degradation pathways, it has been argued that this thioester is a branchpoint for anaerobic and aerobic pathways and that the evolution of oxidative catabolic pathways retained the vestiges of anaerobic processes, activated by CoA addition [73].

## 4. Discussion

This paper describes the natural diversity of group A FPMOs that are involved in the aerobic microbial catabolism of 4-HB. Fig. 11 summarizes the different routes through which 4-HB becomes oxidatively functionalized, so that the resulting products can be ring-cleaved by an intra- or extra-diol dioxygenase.

Most aerobic bacteria make use of PHBH, the prototype group A FPMO, which produces the central intermediate PCA. A subset of aerobic bacteria, however, activate 4-HB through the PhgC-catalyzed formation of 4-hydroxybenzoyl-CoA [69]. This compound subsequently is hydroxylated in a NIH shift type of reaction by PhgA to give gentisyl-CoA. Upon hydrolysis by thioesterase PhgB, this results in the central intermediate GA. Up to now, there is little information about the structure-function relationship of PhgA. Our phylogenetic analysis of (partially) characterized group A enzymes (Fig. S2) suggests that PhgA is closely related to a number of phenolic hydroxylases with unknown 3D-structure. Currently, little can be said about the mode of substrate binding of the large 4-hydroxybenzoyl-CoA molecule and the mechanistic details of the NIH shift reaction remain to be determined.

Fungi and yeasts use alternative ways for the catabolism of 4-HB. One route that leads to PCA and is conserved in ascomycetes involves the action of PhhA [43]. Here we show that this group A FPMO is structurally quite different from PHBH and more related to PHHY and 3HB4H. The active site model of PhhA (Fig. 6) suggests an important role for Asp49 and Tyr242 in substrate activation, whereas Thr111 and Lys219 might fix and orient the substrate via an ionic interaction with the carboxylate moiety of 4-HB. With many polar residues located in the substrate-binding pocket, characterization of the precise mode of substrate binding of PhhA has to await the elucidation of the crystal structure of the enzyme-substrate complex. In the meantime, site-directed mutagenesis of critical active site residues of PhhA (Fig. 6) might give clues about its mechanism of substrate activation and the functional relationship with PHHY and 3HB4H.

Another route of 4-HB oxygenation in eukaryotic microrganisms involves the action of 4HB1H. This FPMO, first isolated from *C. parapsilosis* ([32], catalyzes an oxidative decarboxylation reaction

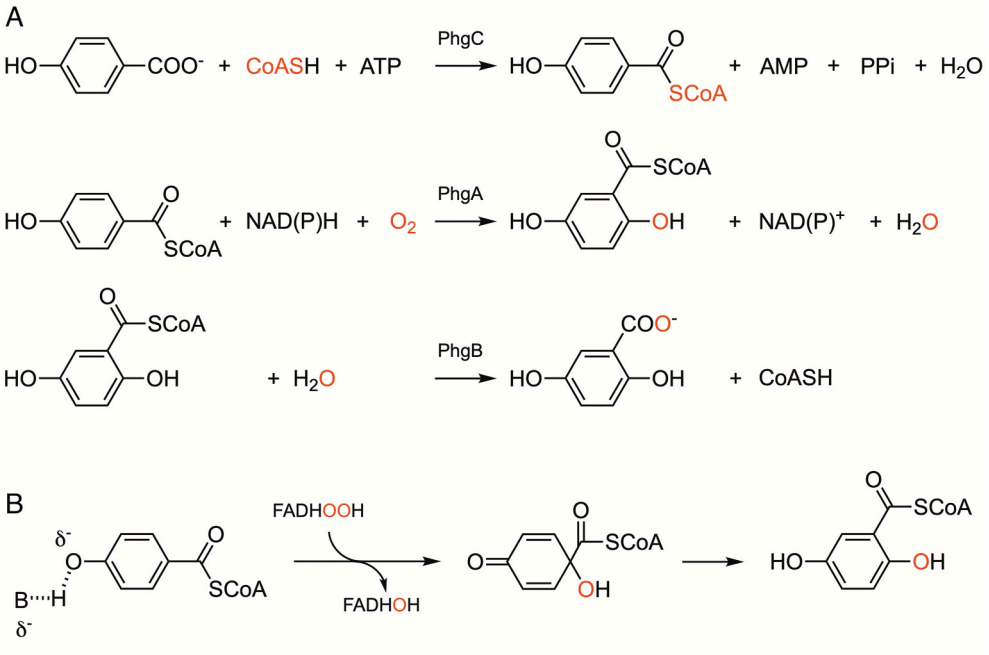


**Fig. 10.** Catabolism of 4-HB to GA in *B. laterosporus* PHB-7a. A) In the first step, 4-HB is converted by PhgC to 4-hydroxybenzoyl-CoA. Next, 4-hydroxybenzoyl-CoA is converted by the NAD(P)H-dependent PhgA to gentisyl-CoA. In the final step, PhgB catalyzes the hydrolysis of gentisyl-CoA to GA. B) Proposed reaction scheme for the flavin-hydroperoxide stimulated hydroxylation of 4-hydroxybenzoyl-CoA to gentisyl-CoA by PhgA [69].

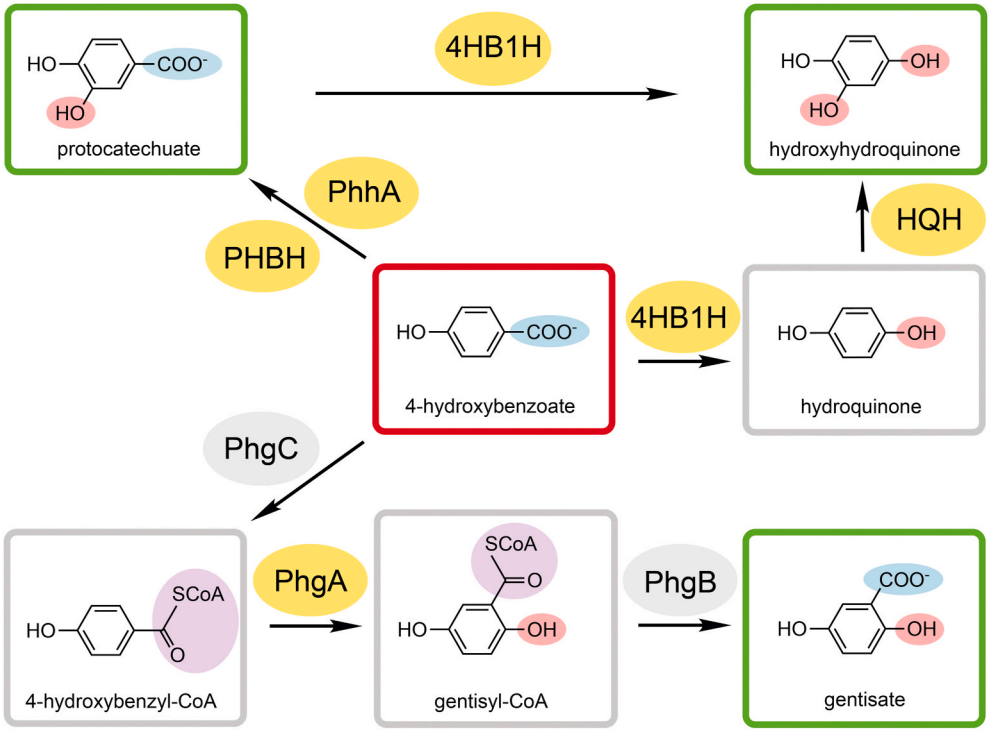


**Fig. 11.** Schematic presentation of the aerobic microbial catabolism of 4-HB. Group A FPMOs that catalyze the hydroxylation of 4-HB (red box) or follow-up steps are depicted as yellow ovals. Introduced hydroxyl groups are shown with a red, carboxylic groups with a blue and SCoA groups with a purple background color. Resulting ring-fission substrates are indicated with a green box and intermediate products with a grey box. Abbreviations are explained in the legend of Table 1. (For interpretation of the references to color in this figure legend, the reader is referred to the Web version of this article.)

yielding HQ. The latter compound has been shown to act as ring-fission substrate in certain proteobacteria [74]. In *C. parapsilosis*, however, HQ is further converted to HHQ by the action of HQH. Interestingly, in this ascomycetous yeast, 4HB1H can also be induced by PCA [32] and convert this compound directly into the central intermediate HHQ (Fig. 11) [50].

The fact that 4HB1H couples the reduction of its FAD cofactor to the efficient hydroxylation of a wide range of 4-HB derivatives including vanillate [50], stimulated us to clone the 4HB1H gene and produce the enzyme in recombinant form. Although a rather good protein expression was achieved, the purified enzyme suffered from FAD loss and did not yield well diffracting crystals. Improving the 4HB1H protein characteristics are needed to remove these barriers in order to facilitate an in-depth structure-function analysis of the 4HB1H active site. Phylogenetic analysis (Fig. 3) and protein homology modelling (Fig. 9) made us conclude that 4HB1H belongs to a subgroup of structurally related group A FPMOs that catalyze *para*-hydroxylation reactions (Fig. S2). Nevertheless, the amino acid residue(s) responsible for the proper binding and activation of 4-HB and its derivatives remain to be elucidated.

Genome mining revealed that 4HB1H is only present in a small group of saccharomycetes. However, we noted that many FAD-binding proteins with unknown function in pezizomycetes and agaricomycetes have structural features in common with 4HB1H, but lack its C-terminal tail. Both from a lignin degradation and enzyme mechanistic point of view it is of high relevance to find out if these 4HB1H lookalikes (Fig. S6 and Fig. S7) are indeed responsible for the predicted V1H activities in these fungal strains.

This paper reports a phylogenetic analysis of 88 functionally characterized group A FPMOs. From the results shown in Fig. S2, it can be concluded that a number of enzymes with similar type of oxygenation chemistry cluster together. This holds for the epoxidases involved in natural product biosynthesis, and for the enzymes that catalyze oxidative dearomatization reactions. Group A FPMOs involved in the biosynthesis of antibiotics are more widely distributed, but most of them are localized in the upper part of the tree (left part in Fig. 3). The phenolic hydroxylases involved in lignin degradation and microbial detoxification mechanisms make up about half of the currently known group A FPMOs. They are found in different parts of the tree, as is the case for the 4-hydroxybenzoate hydroxylases discussed here. The phylogenetic tree also shows no subdivision in taxonomy groups, which means that similar group A FPMOs are not just present within a certain genus. Hence, these flavoenzymes and corresponding reactions are found distributed among several genera, indicative for horizontal gene transfer between species.

In summary, we have introduced in this manuscript several less known group A FPMOs that are involved in the aerobic microbial catabolism of 4-HB. Using sequence alignments and protein homology modelling, we have gained more insight into their mode of action and mutual structural relationship, which allowed us to address some challenges for future research. A phylogenetic analysis of the complete group A FPMO family has learned that the main enzymes discussed here, PHBH, PhhA, 4HB1H, and PhgA, reside in distinct branches of the phylogenetic tree, indicating that they separately diverged from a common ancestor. With this knowledge in hand, it will be of interest to learn more about the origin of these flavoenzymes through ancestral-sequence reconstruction [75].

## Funding

This work was supported in part by a grant from the Federal Ministry for Innovation, Science and Research of North Rhine–Westphalia, Germany (PtJ-TRI/1411ng006)—ChemBioCat. (to D.T).

## CRediT authorship contribution statement

**Adrie H. Westphal:** Methodology, Data curation, Writing – review & editing, Investigation, Software, Validation. **Dirk Tischler:** Methodology, Validation, Writing – review & editing. **Willem J.H. van Berkel:** Conceptualization, Methodology, Data curation, Writing – original draft, Supervision.

## Declaration of competing interest

The authors declare no conflict of interest.

## Acknowledgements

The authors would like to thank Marie Hennebelle (Laboratory of Food Chemistry, Wageningen University & Research) for lipid analysis.

## Appendix B. Supplementary data

Supplementary data to this article can be found online at https://doi.org/10.1016/j.abb.2021.108820.

## Declaration of conflicts of interest

None.

On behalf of all authors, Sincerely yours,

## References

[1] J. Ralph, K. Lundquist, G. Brunow, F. Lu, H. Kim, P.F. Schatz, J.M. Marita, R. D. Hatfield, S.A. Ralph, J.H. Christensen, W. Boerjan, Lignins: natural polymers from oxidative coupling of 4-hydroxyphenyl-propanoids, Phytochemistry Rev. 3 (2004) 29–60, https://doi.org/10.1023/B:PHYT.0000047809.65444.a4.

[2] F.J. Ruiz-Dueñas, A.T. Martínez, Microbial degradation of lignin: how a bulky recalcitrant polymer is efficiently recycled in nature and how we can take advantage of this, Microb. Biotechnol. 2 (2009) 164–177, https://doi.org/10.1111/j.1751-7915.2008.00078.x.

[3] T.D. Bugg, M. Ahmad, E.M. Hardiman, R. Rahmanpour, Pathways for degradation of lignin in bacteria and fungi, Nat. Prod. Rep. 28 (2011) 1883–1896, https://doi.org/10.1039/c1np00042j.

[4] G. Janusz, A. Pawlik, J. Sulej, U. Swiderska-Burek, A. Jarosz-Wilkolazka, A. Paszczynski, Lignin degradation: microorganisms, enzymes involved, genomes analysis and evolution, FEMS Microbiol. Rev. 41 (2017) 941–962, https://doi.org/10.1093/femsre/fux049.

[5] J. Becker, C. Wittmann, A field of dreams: lignin valorization into chemicals, materials, fuels, and health-care products, Biotechnol. Adv. 37 (2019) 107360, https://doi.org/10.1016/j.biotechadv.2019.02.016.

[6] D.P. Brink, K. Ravi, G. Lidén, M.F. Gorwa-Grauslund, Mapping the diversity of microbial lignin catabolism: experiences from the eLignin database, Appl. Microbiol. Biotechnol. 103 (2019) 3979–4002, https://doi.org/10.1007/s00253-019-09692-4.

[7] G. van Erven, J. Wang, P. Sun, P. de Waard, J. van der Putten, G.E. Frissen, R.J. A. Gosselink, G. Zinovyev, A. Potthast, W.J.H. van Berkel, M.A. Kabel, Structural motifs of wheat straw lignin differ in susceptibility to degradation by the white-rot fungus *Ceriporiopsis subvermispora*, ACS Sustain. Chem. Eng. 7 (2019) 20032–20042, https://doi.org/10.1021/acssuschemeng.9b05780.

[8] C.S. Harwood, R.E. Parales, The β-ketoadipate pathway and the biology of self-identity, Annu. Rev. Microbiol. 50 (1996) 553–590, https://doi.org/10.1146/annurev.micro.50.1.553.

[9] O.Y. Abdelaziz, D.P. Brink, J. Prothmann, K. Ravi, M. Sun, J. García-Hidalgo, M. Sandahl, C.P. Hulteberg, C. Turner, G. Lidén, M.F. Gorwa-Grauslund, Biological valorization of low molecular weight lignin, Biotechnol. Adv. 34 (2016) 1318–1346, https://doi.org/10.1016/j.biotechadv.2016.10.001.

[10] R.J.M. Lubbers, A. Dilokpimol, J. Visser, M.R. Mäkelä, K.S. Hildén, R.P. de Vries, A comparison between the homocyclic aromatic metabolic pathways from plant-derived compounds by bacteria and fungi, Biotechnol. Adv. 37 (2019) 107396, https://doi.org/10.1016/j.biotechadv.2019.05.002.

[11] A.J. Ragauskas, G.T. Beckham, M.J. Biddy, R. Chandra, F. Chen, M.F. Davis, B. H. Davison, R.A. Dixon, P. Gilna, M. Keller, P. Langan, A.K. Naskar, J.N. Saddler, T. J. Tschaplinski, G.A. Tuskan, C.E. Wyman, Lignin valorization: improving lignin processing in the Biorefinery, Science 344 (2014) 1246843, https://doi.org/10.1126/science.1246843.

[12] A.T. Martínez, F.J. Ruiz-Dueñas, S. Camarero, A. Serrano, D. Linde, H. Lund, J. Vind, M. Tovborg, O.M. Herold-Majumdar, M. Hofrichter, C. Liers, R. Ullrich, K. Scheibner, G. Sannia, A. Piscitelli, C. Pezzella, M.E. Sener, S. Kılıç, W.J.H. van Berkel, V.i. Guallar, M.F. Lucas, R. Zuhse, R. Ludwig, F. Hollmann, E. Fernández-Fueyo, E. Record, C.B. Faulds, M. Tortajada, I. Winckelmann, J.-A. Rasmussen, M. Gelo-Pujic, A. Gutiérrez, J.C. Del Río, J. Rencoret, M. Alcalde, Oxidoreductases on their way to industrial biotransformations, Biotechnol. Adv. 35 (2017) 815–831, https://doi.org/10.1016/j.biotechadv.2017.06.003.

[13] G. van Erven, A.F. Kleijn, A. Patyshakuliyeva, M. Di Falco, A. Tsang, R.P. de Vries, W.J.H. van Berkel, M.A. Kabel, Evidence for ligninolytic activity of the ascomycete fungus *Podospora anserina*, Biotechnol. Biofuels 13 (2020) 75, https://doi.org/10.1186/s13068-020-01713-z.

[14] T.D.H. Bugg, M. Ahmad, E.M. Hardiman, R. Singh, The emerging role for bacteria in lignin degradation and bio-product formation, Curr. Opin. Biotechnol. 22 (2011) 394–400, https://doi.org/10.1016/j.copbio.2010.10.009.

[15] J.C. del Río, J. Rencoret, A. Gutiérrez, T. Elder, H. Kim, J. Ralph, Lignin monomers from beyond the canonical monolignol biosynthetic pathway: another brick in the wall, ACS Sustain. Chem. Eng. 8 (2020) 4997–5012, https://doi.org/10.1021/acssuschemeng.0c01109.

[16] K. Hosokawa, R.Y. Stanier, Crystallization and properties of *p*-hydroxybenzoate hydroxylase from *Pseudomonas putida*, J. Biol. Chem. 241 (1966) 2453–2460.

[17] B. Seibold, M. Matthes, M.H.M. Eppink, F. Lingens, W.J.H. van Berkel, R. Muller, 4-Hydroxybenzoate hydroxylase from *Pseudomonas* sp. CBS3. Purification, characterization, gene cloning, sequence analysis and assignment of structural features determining the coenzyme specificity, Eur. J. Biochem. 239 (1996) 469–478, https://doi.org/10.1111/j.1432-1033.1996.0469u.x.

[18] R.K. Wierenga, R.J. de Jong, K.H. Kalk, W.G. Hol, J. Drenth, Crystal structure of *p*-hydroxybenzoate hydroxylase, J. Mol. Biol. 131 (1979) 55–73, https://doi.org/10.1016/0022-2836(79)90301-2.

[19] H.A. Schreuder, P.A.J. Prick, R.K. Wierenga, G. Vriend, K.S. Wilson, W.G.J. Hol, J. Drenth, Crystal structure of the *p*-hydroxybenzoate hydroxylase-substrate complex refined at 1.9 Å resolution: analysis of the enzyme-substrate and enzyme-product complexes, J. Mol. Biol. 208 (1989) 679–696, https://doi.org/10.1016/0022-2836(89)90158-7.

[20] B. Entsch, W.J.H. Van Berkel, Structure and mechanism of *para*-hydroxybenzoate hydroxylase, Faseb. J. 9 (1995) 476–483, https://doi.org/10.1096/fasebj.9.7.7737455.

[21] B. Entsch, L.J. Cole, D.P. Ballou, Protein dynamics and electrostatics in the function of *p*-hydroxybenzoate hydroxylase, Arch. Biochem. Biophys. 433 (2005) 297–311, https://doi.org/10.1016/j.abb.2004.09.029.

[22] B.A. Palfey, C.A. McDonald, Control of catalysis in flavin-dependent monooxygenases, Arch. Biochem. Biophys. 493 (2010) 26–36, https://doi.org/10.1016/j.abb.2009.11.028.

[23] K. Crozier-Reabe, G.R. Moran, Form follows function: structural and catalytic variation in the Class A flavoprotein monooxygenases, Int. J. Mol. Sci. 13 (2012), https://doi.org/10.3390/ijms131215601.

[24] M.L. Mascotti, M. Juri Ayub, N. Furnham, J.M. Thornton, R.A. Laskowski, Chopping and changing: the evolution of the flavin-dependent monooxygenases, J. Mol. Biol. 428 (2016) 3131–3146, https://doi.org/10.1016/j.jmb.2016.07.003.

[25] B.A. Palfey, G.R. Moran, B. Entsch, D.P. Ballou, V. Massey, Substrate recognition by "password" in *p*-hydroxybenzoate hydroxylase, Biochemistry 38 (1999) 1153–1158, https://doi.org/10.1021/bi9826613.

[26] W.J.H. van Berkel, N.M. Kamerbeek, M.W. Fraaije, Flavoprotein monooxygenases, a diverse class of oxidative biocatalysts, J. Biotechnol. 124 (2006) 670–689, https://doi.org/10.1016/j.jbiotec.2006.03.044.

[27] M.M.E. Huijbers, S. Montersino, A.H. Westphal, D. Tischler, W.J.H. van Berkel, Flavin dependent monooxygenases, Arch. Biochem. Biophys. 544 (2014) 2–17, https://doi.org/10.1016/j.abb.2013.12.005.

[28] C.E. Paul, D. Eggerichs, A.H. Westphal, D. Tischler, W.J.H. van Berkel, Flavoprotein monooxygenases: versatile biocatalysts, Biotechnol. Adv. (2021), https://doi.org/10.1016/j.biotechadv.2021.107712.

[29] A.H. Westphal, D. Tischler, F. Heinke, S. Hofmann, J.A.D. Gröning, D. Labudde, W. J.H. van Berkel, Pyridine nucleotide coenzyme specificity of *p*-hydroxybenzoate hydroxylase and related flavoprotein monooxygenases, Front. Microbiol. 9 (2018) 10, https://doi.org/10.3389/fmicb.2018.03050.

[30] S. Montersino, R. Orru, A. Barendregt, A.H. Westphal, E. van Duijn, A. Mattevi, W. J.H. van Berkel, Crystal structure of 3-hydroxybenzoate 6-hydroxylase uncovers lipid-assisted flavoprotein strategy for regioselective aromatic hydroxylation, J. Biol. Chem. 288 (2013) 26235–26245, https://doi.org/10.1074/jbc.M113.479303.

[31] S. Montersino, E. te Poele, R. Orru, A.H. Westphal, A. Barendregt, A.J.R. Heck, R. van der Geize, L. Dijkhuizen, A. Mattevi, W.J.H. van Berkel, 3-Hydroxybenzoate 6-hydroxylase from *Rhodococcus jostii* RHA1 contains a phosphatidylinositol cofactor, Front. Microbiol. 8 (2017) 11, https://doi.org/10.3389/fmicb.2017.01110.

[32] W.J.H. van Berkel, M.H.M. Eppink, W.J. Middelhoven, J.M. Vervoort, I.M.C. M. Rietjens, Catabolism of 4-hydroxybenzoate in *Candida parapsilosis* proceeds through initial oxidative decarboxylation by a FAD-dependent 4-hydroxybenzoate 1-hydroxylase, FEMS Microbiol. Lett. 121 (1994) 207–215, https://doi.org/10.1111/j.1574-6968.1994.tb07100.x.

[33] S. Kumar, G. Stecher, K. Tamura, MEGA7: molecular evolutionary genetics analysis version 7.0 for bigger datasets, Mol. Biol. Evol. 33 (2016) 1870–1874, https://doi.org/10.1093/molbev/msw054.

[34] N. Saitou, M. Nei, The neighbor-joining method: a new method for reconstructing phylogenetic trees, Mol. Biol. Evol. 4 (1987) 406–425, https://doi.org/10.1093/oxfordjournals.molbev.a040454.

[35] D.T. Jones, W.R. Taylor, J.M. Thornton, The rapid generation of mutation data matrices from protein sequences, Bioinformatics 8 (1992) 275–282, https://doi.org/10.1093/bioinformatics/8.3.275.

[36] J. Felsenstein, Confidence limits on phylogenies: an approach using the bootstrap, Evolution 39 (1985) 783–791, https://doi.org/10.2307/2408678.

[37] J. Pei, B.-H. Kim, N.V. Grishin, PROMALS3D: a tool for multiple protein sequence and structure alignments, Nucleic Acids Res. 36 (2008) 2295–2300, https://doi.org/10.1093/nar/gkn072.

[38] A. Šali, T.L. Blundell, Comparative protein modelling by satisfaction of spatial restraints, J. Mol. Biol. 234 (1993) 779–815, https://doi.org/10.1006/jmbi.1993.1626.

[39] N. Eswar, B. Webb, M.A. Marti-Renom, M.S. Madhusudhan, D. Eramian, M.-Y. Shen, U. Pieper, A. Sali, Comparative protein structure modeling using MODELLER, Curr. Protein Pept. Sci. (2007), https://doi.org/10.1002/0471140864.ps0209s50 (Chapter 2), Unit 2.9.

[40] L.L.C. Schrodinger, The PyMOL Molecular Graphics System, Version 1.8, 2015.

[41] R.-J. Hung, U. Yazdani, J. Yoon, H. Wu, T. Yang, N. Gupta, Z. Huang, W.J.H. van Berkel, J.R. Terman, Mical links semaphorins to F-actin disassembly, Nature 463 (2010) 823–827, https://doi.org/10.1038/nature08724.

[42] T.M. Martins, D.O. Hartmann, S. Planchon, I. Martins, J. Renaut, C. Silva Pereira, The old 3-oxoadipate pathway revisited: new insights in the catabolism of

aromatics in the saprophytic fungus *Aspergillus nidulans*, Fungal Genet. Biol. 74 (2015) 32–44, https://doi.org/10.1016/j.fgb.2014.11.002.
[43] R.J.M. Lubbers, A. Dilokpimol, M. Peng, J. Visser, M.R. Mäkelä, K.S. Hildén, R. P. de Vries, Discovery of novel *p*-hydroxybenzoate-*m*-hydroxylase, protocatechuate 3,4 ring-cleavage dioxygenase, and hydroxyquinol 1,2 ring-cleavage dioxygenase from the filamentous fungus *Aspergillus niger*, ACS Sustain. Chem. Eng. 7 (2019) 19081–19089, https://doi.org/10.1021/acssuschemeng.9b04918.
[44] C. Enroth, H. Neujahr, G. Schneider, Y. Lindqvist, The crystal structure of phenol hydroxylase in complex with FAD and phenol provides evidence for a concerted conformational change in the enzyme and its cofactor during catalysis, Structure 6 (1998) 605–617, https://doi.org/10.1016/S0969-2126(98)00062-8.
[45] C. Enroth, High-resolution structure of phenol hydroxylase and correction of sequence errors, Acta Crystallogr. D 59 (2003) 1597–1602, https://doi.org/10.1107/S0907444903014902.
[46] T. Hiromoto, S. Fujiwara, K. Hosokawa, H. Yamaguchi, Crystal structure of 3-hydroxybenzoate hydroxylase from *Comamonas testosteroni* has a large tunnel for substrate and oxygen access to the active site, J. Mol. Biol. 364 (2006) 878–896, https://doi.org/10.1016/j.jmb.2006.09.031.
[47] D. Xu, D.P. Ballou, V. Massey, Studies of the mechanism of phenol hydroxylase: mutants Tyr289Phe, Asp54Asn, and Arg281Met, Biochemistry 40 (2001) 12369–12378, https://doi.org/10.1021/bi010962y.
[48] H.K. Chang, G.J. Zylstra, Examination and expansion of the substrate range of *m*-hydroxybenzoate hydroxylase, Biochem. Biophys. Res. Commun. 371 (2008) 149–153, https://doi.org/10.1016/j.bbrc.2008.04.032.
[49] H.Y. Neujahr, A. Gaal, Phenol hydroxylase from yeast, Eur. J. Biochem. 35 (1973) 386–400, https://doi.org/10.1111/j.1432-1033.1973.tb02851.x.
[50] M.H.M. Eppink, S.A. Boeren, J.M. Vervoort, W.J.H. van Berkel, Purification and properties of 4-hydroxybenzoate 1-hydroxylase (decarboxylating), a novel flavin adenine dinucleotide-dependent monooxygenase from *Candida parapsilosis* CBS604, J. Bacteriol. 179 (1997) 6680–6687, https://doi.org/10.1128/jb.179.21.6680-6687.1997.
[51] M.H.M. Eppink, E. Cammaart, D. van Wassenaar, W.J. Middelhoven, W.J.H. van Berkel, Purification and properties of hydroquinone hydroxylase, a FAD-dependent monooxygenase involved in the catabolism of 4-hydroxybenzoate in *Candida parapsilosis* CBS604, Eur. J. Biochem. 267 (2000) 6832–6840, https://doi.org/10.1046/j.1432-1033.2000.01783.x.
[52] G. Butler, M.D. Rasmussen, M.F. Lin, M.A.S. Santos, S. Sakthikumar, C.A. Munro, E. Rheinbay, M. Grabherr, A. Forche, J.L. Reedy, I. Agrafioti, M.B. Arnaud, S. Bates, A.J.P. Brown, S. Brunke, M.C. Costanzo, D.A. Fitzpatrick, P.W.J. de Groot, D. Harris, L.L. Hoyer, B. Hube, F.M. Klis, C. Kodira, N. Lennard, M.E. Logue, R. Martin, A.M. Neiman, E. Nikolaou, M.A. Quail, J. Quinn, M.C. Santos, F. F. Schmitzberger, G. Sherlock, P. Shah, K.A.T. Silverstein, M.S. Skrzypek, D. Soll, R. Staggs, I. Stansfield, M.P.H. Stumpf, P.E. Sudbery, T. Srikantha, Q. Zeng, J. Berman, M. Berriman, J. Heitman, N.A.R. Gow, M.C. Lorenz, B.W. Birren, M. Kellis, C.A. Cuomo, Evolution of pathogenicity and sexual reproduction in eight *Candida* genomes, Nature 459 (2009) 657–662, https://doi.org/10.1038/nature08064.
[53] Z. Holesova, M. Jakubkova, I. Zavadiakova, I. Zeman, L. Tomaska, J. Nosek, Gentisate and 3-oxoadipate pathways in the yeast *Candida parapsilosis*: identification and functional analysis of the genes coding for 3-hydroxybenzoate 6-hydroxylase and 4-hydroxybenzoate 1-hydroxylase, Microbiology 157 (2011) 2152–2163, https://doi.org/10.1099/mic.0.048215-0.
[54] G. Gérecová, M. Neboháčová, I. Zeman, L.P. Pryszcz, Ľ. Tomáška, T. Gabaldón, J. Nosek, Metabolic gene clusters encoding the enzymes of two branches of the 3-oxoadipate pathway in the pathogenic yeast *Candida albicans*, FEMS Yeast Res. 15 (2015), https://doi.org/10.1093/femsyr/fov006.
[55] T. Uemura, A. Kita, Y. Watanabe, M. Adachi, R. Kuroki, Y. Morimoto, The catalytic mechanism of decarboxylative hydroxylation of salicylate hydroxylase revealed by crystal structure analysis at 2.5 Å resolution, Biochem. Biophys. Res. Commun. 469 (2016) 158–163, https://doi.org/10.1016/j.bbrc.2015.11.087.
[56] D.M.A. Costa, S.V. Gómez, S.S. de Araújo, M.S. Pereira, R.B. Alves, D.C. Favaro, A. C. Hengge, R.A.P. Nagem, T.A.S. Brandão, Catalytic mechanism for the conversion of salicylate into catechol by the flavin-dependent monooxygenase salicylate hydroxylase, Int. J. Biol. Macromol. 129 (2019) 588–600, https://doi.org/10.1016/j.ijbiomac.2019.01.135.
[57] J. Sucharitakul, D. Medhanavyn, D. Pakotiprapha, W.J.H. van Berkel, P. Chaiyen, Tyr217 and His213 are important for substrate binding and hydroxylation of 3-hydroxybenzoate 6-hydroxylase from *Rhodococcus jostii* RHA1, FEBS J. 283 (2016) 860–881, https://doi.org/10.1111/febs.13636.
[58] W. Pitsawong, P. Chenprakhon, T. Dhammaraj, D. Medhanavyn, J. Sucharitakul, C. Tongsook, W.J.H. van Berkel, P. Chaiyen, A.-F. Miller, Tuning of p*K*a values activates substrates in flavin-dependent aromatic hydroxylases, J. Biol. Chem. 295 (2020) 3965–3981, https://doi.org/10.1074/jbc.RA119.011884.
[59] K.D. Nakamoto, S.W. Perkins, R.G. Campbell, M.R. Bauerle, T.J. Gerwig, S. Gerislioglu, C. Wesdemiotis, M.A. Anderson, K.A. Hicks, M.J. Snider, Mechanism of 6-hydroxynicotinate 3-monooxygenase, a flavin-dependent decarboxylative hydroxylase involved in bacterial nicotinic acid degradation, Biochemistry 58 (2019) 1751–1763, https://doi.org/10.1021/acs.biochem.8b00969.
[60] K.A. Hicks, M.E. Yuen, W.F. Zhen, T.J. Gerwig, R.W. Story, M.C. Kopp, M.J. Snider, Structural and biochemical characterization of 6-hydroxynicotinic acid 3-monooxygenase, a novel decarboxylative hydroxylase involved in aerobic nicotinate degradation, Biochemistry 55 (2016) 3432–3446, https://doi.org/10.1021/acs.biochem.6b00105.
[61] T.K. Kirk, L.F. Lorenz, Oxygenation of 4-alkoxyl groups in alkoxybenzoic acids by *Polyporus dichrous*, Appl. Microbiol. 27 (1974) 360–367.
[62] Y. Yajima, A. Enoki, M.B. Mayfield, M.H. Gold, Vanillate hydroxylase from the white rot basidiomycete *Phanerochaete chrysosporium*, Arch. Microbiol. 123 (1979) 319–321, https://doi.org/10.1007/BF00406669.
[63] J.A. Buswell, K.-E. Eriksson, J.K. Gupta, S.G. Hamp, I. Nordh, Vanillic acid metabolism by selected soft-rot, brown-rot, and white-rot fungi, Arch. Microbiol. 131 (1982) 366–374, https://doi.org/10.1007/BF00411188.
[64] J.A. Buswell, K.-E. Eriksson, B. Pettersson, Purification and partial characterization of vanillate hydroxylase (decarboxylating) from *Sporotrichum pulverulentum*, J. Chromatogr., A 215 (1981) 99–108, https://doi.org/10.1016/S0021-9673(00)81390-4.
[65] Y.-L. Yang, H. Zhou, G. Du, K.-N. Feng, T. Feng, X.-L. Fu, J.-K. Liu, Y. Zeng, A monooxygenase from *Boreostereum vibrans* catalyzes oxidative decarboxylation in a divergent vibralactone biosynthesis pathway, Angew. Chem. Int. Ed. 55 (2016) 5463–5466, https://doi.org/10.1002/anie.201510928.
[66] K. Chen, Y. Mu, S. Jian, X. Zang, Q. Chen, W. Jia, Z. Ke, Y. Gao, J. Jiang, Comparative transcriptome analysis reveals the mechanism underlying 3,5-dibromo-4-hydroxybenzoate catabolism via a new oxidative decarboxylation pathway, Appl. Environ. Microbiol. 84 (2018), e02467-02417, https://doi.org/10.1128/AEM.02467-17.
[67] R.L. Crawford, Pathways of 4-hydroxybenzoate degradation among species of *Bacillus*, J. Bacteriol. 127 (1976) 204–210, https://doi.org/10.1128/JB.127.1.204-210.1976.
[68] D.J. Fairley, D.R. Boyd, N.D. Sharma, C.C.R. Allen, P. Morgan, M.J. Larkin, Aerobic metabolism of 4-hydroxybenzoic acid in Archaea via an unusual pathway involving an intramolecular migration (NIH Shift), Appl. Environ. Microbiol. 68 (2002) 6246, https://doi.org/10.1128/AEM.68.12.6246-6255.2002.
[69] H. Zhao, Y. Xu, S. Lin, J.C. Spain, N.-Y. Zhou, The molecular basis for the intramolecular migration (NIH shift) of the carboxyl group during para-hydroxybenzoate catabolism, Mol. Microbiol. 110 (2018) 411–424, https://doi.org/10.1111/mmi.14094.
[70] W.A. Hareland, R.L. Crawford, P.J. Chapman, S. Dagley, Metabolic function and properties of 4-hydroxyphenylacetic acid 1-hydroxylase from *Pseudomonas acidovorans*, J. Bacteriol. 121 (1975) 272, https://doi.org/10.1128/JB.121.1.272-285.1975.
[71] L.-K. Liu, H. Abdelwahab, J.S. Martin Del Campo, R. Mehra-Chaudhary, P. Sobrado, J.J. Tanner, The structure of the antibiotic deactivating, *N*-hydroxylating rifampicin monooxygenase, J. Biol. Chem. 291 (2016) 21553–21562, https://doi.org/10.1074/jbc.M116.745315.
[72] K. Koteva, G. Cox, J.K. Kelso, M.D. Surette, H.L. Zubyk, L. Ejim, P. Stogios, A. Savchenko, D. Sørensen, G.D. Wright, Rox, a rifamycin resistance enzyme with an unprecedented mechanism of action, Cell Chem. Biol. 25 (2018) 403–412, https://doi.org/10.1016/j.chembiol.2018.01.009, e405.
[73] G. Fuchs, M. Boll, J. Heider, Microbial degradation of aromatic compounds - from one strategy to four, Nat. Rev. Microbiol. 9 (2011) 803–816, https://doi.org/10.1038/nrmicro2652.
[74] M.J.H. Moonen, N.M. Kamerbeek, A.H. Westphal, S.A. Boeren, D.B. Janssen, M. W. Fraaije, W.J.H. van Berkel, Elucidation of the 4-hydroxyacetophenone catabolic pathway in *Pseudomonas fluorescens* ACB, J. Bacteriol. 190 (2008) 5190–5198, https://doi.org/10.1128/JB.01944-07.
[75] C.R. Nicoll, G. Bailleul, F. Fiorentini, M.L. Mascotti, M.W. Fraaije, A. Mattevi, Ancestral-sequence reconstruction unveils the structural basis of function in mammalian FMOs, Nat. Struct. Mol. Biol. 27 (2020) 14–24, https://doi.org/10.1038/s41594-019-0347-2.